Journal of Geophysical Research: Oceans

Modeling of the Influence of Sea Ice Cycle and Langmuir Circulation on the Upper Ocean Mixed Layer Depth and Freshwater Distribution at the West Antarctic Peninsula

C. Schultz[1], S. C. Doney[1], W. G. Zhang[2], H. Regan[3], P. Holland[4], M. Meredith[4], S. Stammerjohn[5]

[1] University of Virginia, Department of Environmental Sciences, Charlottesville, VA, USA
[2] Woods Hole Oceanographic Institution, Woods Hole, MA, USA
[3] Univ. Brest, CNRS, IRD, Ifremer, Laboratoire D'Océanographie Physique et Spatiale, IUEM, Brest, France
[4] British Antarctic Survey, Natural Environment Research Council, Cambridge, UK
[5] Institute of Arctic and Alpine Research, University of Colorado, Boulder, CO, USA

Corresponding author: Cristina Schultz (cs3xm@virginia.edu)

Contents of this file

Introduction

The data used to make the figures and tables in this document is the same as described in the methods section in the article.

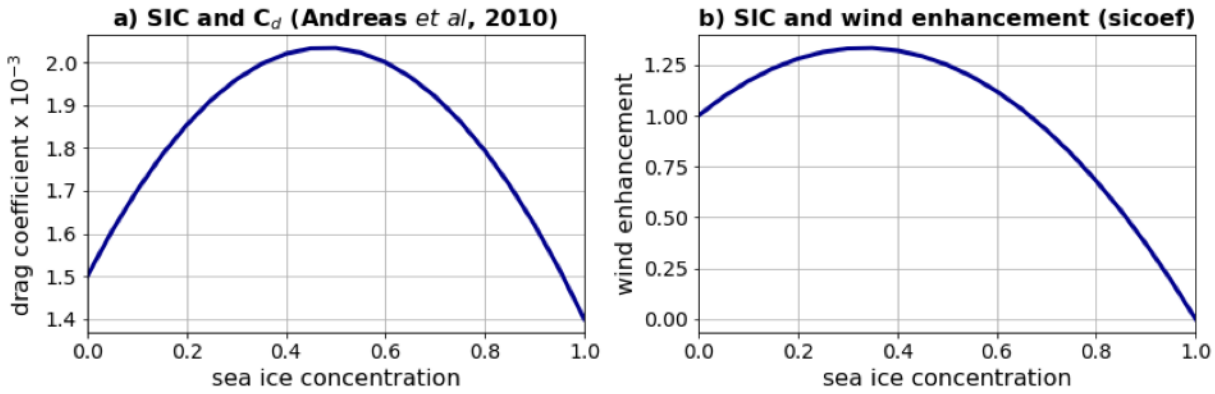

Figure S1: a) Relationship between wind-sea-ice drag coefficient (Cd) and sea ice concentration from Andreas et al (2010); b) Relationship between the wind enhancement factor (sicoef) and sea ice concentration used in this study.

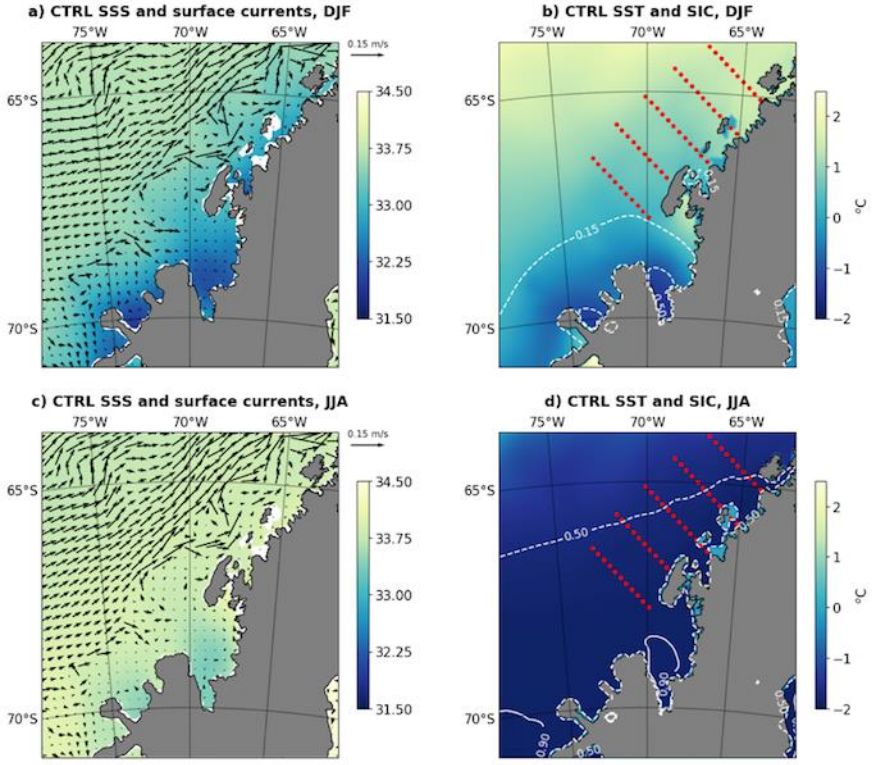

Figure S2: Simulated climatology (from CTRL integration) of A) sea surface salinity (color), surface currents (arrows), B) Sea surface temperature (color) and sea ice concentration (white dashed line) during the summer (December-February); climatology of C) sea surface salinity (color), surface currents (arrows), D) sea surface temperature and sea ice concentration during winter (June-August). The red dots on panels B and D represent the location of the Palmer-LTER cruise stations.

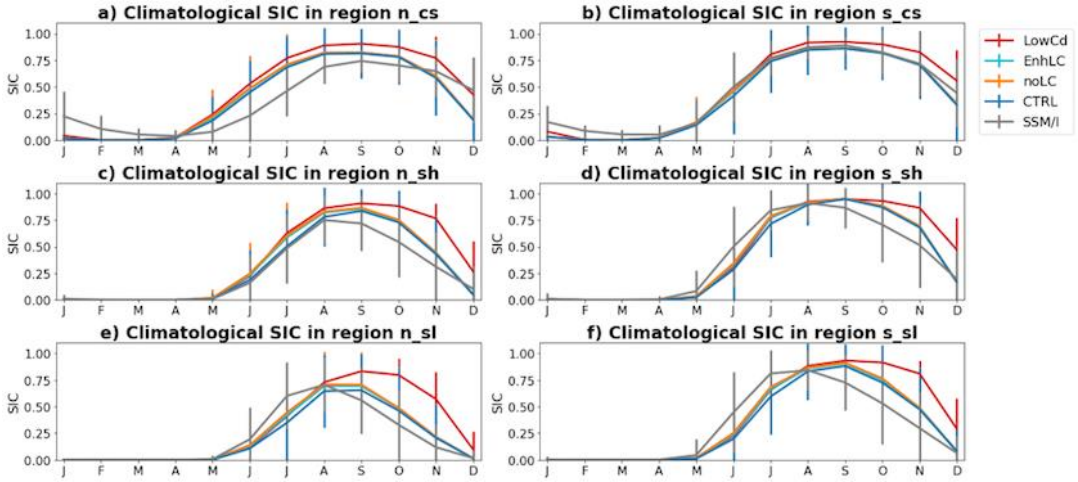

Figure S3: Monthly climatology of sea ice concentration from the satellite observations (SSM/I; grey) and from the model simulations (other color). Vertical bars indicate standard deviation between the monthly means of each year.

Although onset times of sea-ice advance and retreat offer valuable information on the interannual variability of sea-ice dynamics in the region, climatological monthly means of SIC (Figure S3) provides information on how each simulation compares to observations throughout the year. In the northern coastal region, the model showed lower variability compared to the satellite data, evidenced by the lower standard deviation; and had a faster increase and decrease in SIC during advance and retreat of sea ice, leading to higher SIC in the winter and lower in the summer when compared to observations. In the southern coastal region, the model simulation shows a somewhat faster decrease of sea ice during summer months, with lower SIC during January and February, but the advance of sea ice is well captured. In the shelf and slope region, modeled sea-ice retreat happened later than the observed, and although sea-ice advance had a similar start date the observations, the observations had a faster increase of SIC.

Comparing the SIC climatologies from the CTRL and LowCd results, it is seen that lower drag coefficient leads to later sea-ice retreat in all sub-regions. High SIC persists in LowCd well into October (November) in the slope (shelf), with SIC higher than 0.75 while observations and CTRL show concentrations during that period below 0.5. The differences in sea-ice advance are less pronounced. Simulations noLC and EnhLC have similar SIC to LowCd during the season of sea ice advance, suggesting that wind action is not the cause of the SIC discrepancy. Different treatments for LC did not affect the retreat of sea ice, confirming the previous assessment that wind action is more important for retreat of sea ice than for its advance.

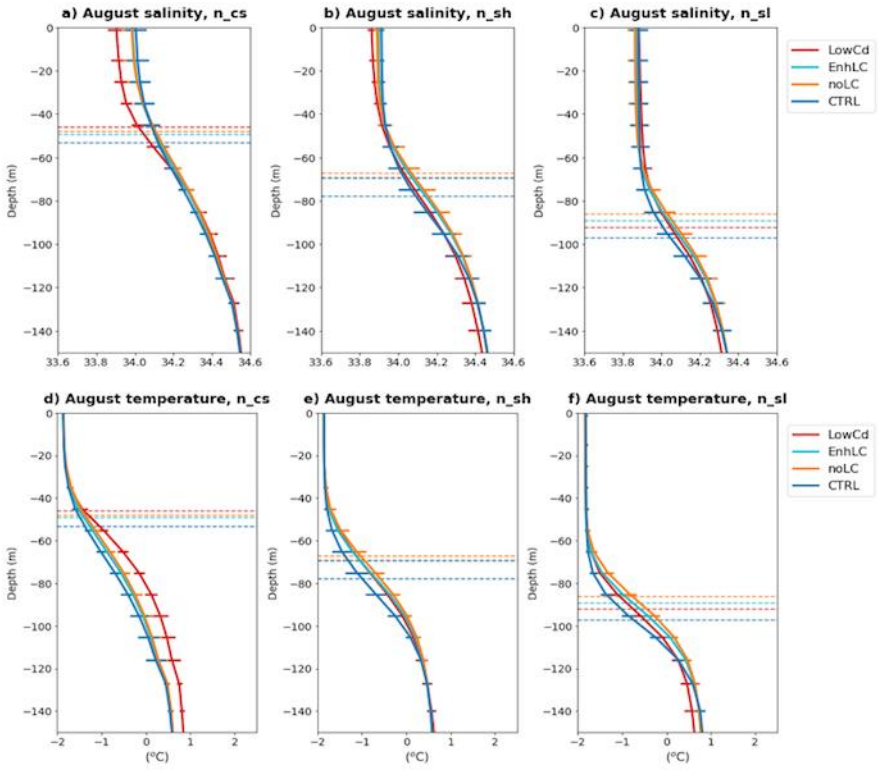

Figure S4: Simulated August salinity climatology for (a) northern coast, (b) northern shelf and (c) northern slope regions; and simulated August climatology of temperature for (d) northern coast, (e) northern shelf and (f) northern slope regions. Horizontal solid lines represent standard deviation, and horizontal dashed lines indicate climatological MLD for the period considered.

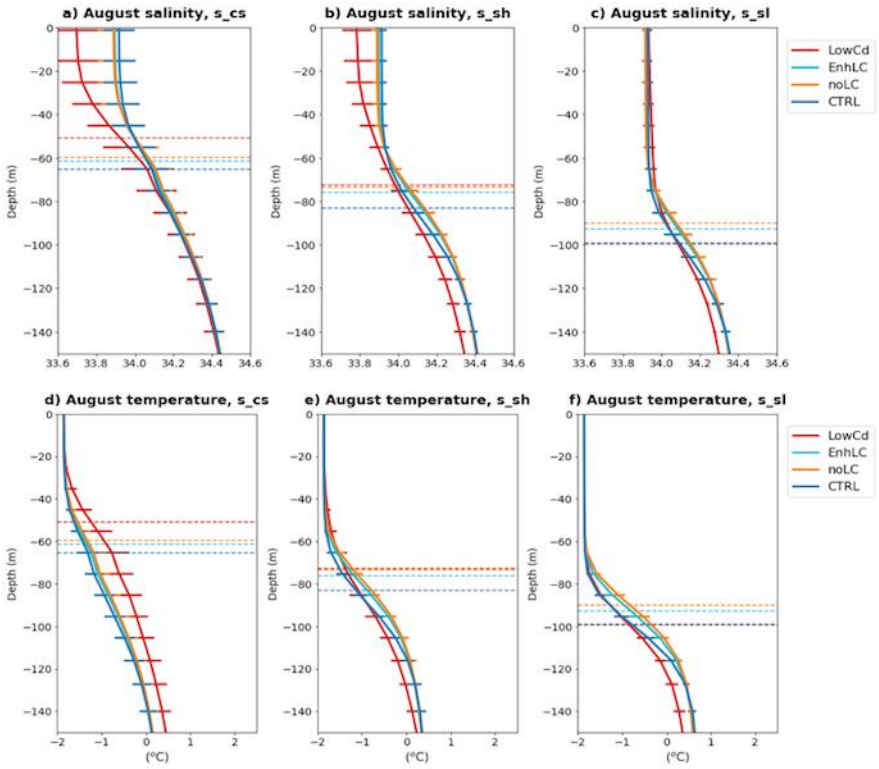

Figure S5: Simulated August climatology of salinity for (a) southern coast, (b) southern shelf and (c) southern slope regions; and simulated August climatology of temperature for (d) southern coast, (e) southern shelf and (f) southern slope regions. Horizontal solid lines represent standard deviation, and horizontal dashed lines indicate climatological MLD for the period considered.

Experiment Name	**Cd**	**LC Parameterization**
CTRL (control simulation)	$2*10^{-3}$	Li and Fox-Kemper (2017)
LowCd (simulation with lower Cd value)	$5*10^{-4}$	Li and Fox-Kemper (2017)
noLC (simulation with no LC parameterization)	$2*10^{-3}$	None
EnhLC (Enhanced LC simulation)	$2*10^{-3}$	Li et al (2017)

Table S1: Values of air-sea ice drag coefficient (*Cd*) and choices of Langmuir circulation parameterization in each simulation.

	s_cs	s_sh	s_sl	n_cs	n_sh	n_sl
CTRL	0.87	0.82	0.92	0.62	0.70	0.86
noLC	0.75	0.88	0.86	0.52	0.72	0.81
LowCd	0.44	0.80	0.92	0.44	0.66	0.81
EnhLC	0.75	0.89	0.85	0.64	0.72	0.80

Table S2: Correlation between modeled and observed times of sea ice advance. All correlations are significant at 95% confidence level. Location of stations for each sub-region are shown in Figure 1B, and description of simulations are shown in Table S1.

	s_cs	**s_sh**	**s_sl**	**n_cs**	**n_sh**	**n_sl**
CTRL	0.87	0.86	0.81	0.89	0.85	0.82
noLC	0.85	0.83	0.75	0.91	0.86	0.79
LowCd	0.51	0.27	0.61	0.67	0.44	0.58
EnhLC	0.85	0.84	0.77	0.91	0.86	0.80

Table S3: Correlation between modeled and observed times of sea ice retreat. All correlations, with the exception of LowCd at s_sh, are significant at 95% confidence level. Location of stations for each sub-region are shown in Figure 1B, and description of simulations are shown in Table S1.

	n_cs	**n_sh**	**n_sl**	**s_cs**	**s_sh**	**s_sl**
CTRL	0.308	0.703	0.596	0.575	0.932	0.110
noLC	0.322	0.580	0.534	0.574	0.843	0.125
LowCd	0.229	0.417	0.486	0.437	0.698	0.170
EnhLC	0.301	0.604	0.554	0.563	0.859	0.142

TableS 4: Correlation coefficient between simulated average MLD for January-February each year and Palmer-LTER average MLD for each cruise in each sub-region. Numbers in bold are significant at 95% confidence level. Location of stations for each sub-region are shown in Figure 1B, and description of simulations are shown in Table S1.